## **Non-premixed Turbulent Combustion**

Jonathan H. Frank and Robert S. Barlow

Combustion Research Facility
Sandia National Laboratories
Livermore, CA 94551

#### Introduction

In non-premixed combustion, the fuel and oxidizer streams are introduced separately, and combustion occurs after the fuel and oxidizer mix on the molecular scale. Many practical combustion devices, such as furnaces, steam boilers, diesel engines, liquid rocket motors, and gas turbine engines, involve turbulent non-premixed combustion. In these devices, mixing occurs by a combination of turbulent stirring of the fuel and oxidizer streams and molecular diffusion. Turbulence greatly enhances the mixing process by increasing the surface area of the thin mixing layers where most of the molecular diffusion occurs. The interaction between turbulent mixing and combustion chemistry is extremely complex and remains an active research area. In this chapter, we provide an overview of some basic characteristics of turbulent non-premixed combustion. The emphasis is on fundamental phenomena that have been experimentally studied in relatively simple burner configurations but are also relevant to the understanding and predictive modeling of complex combustion systems. Detailed treatments of the theory, modeling, and applications of turbulent non-premixed combustion are available elsewhere.<sup>1-5</sup>

#### **Basic Characteristics of Jet Flames**

The structure of non-premixed flames is governed by the coupling between mixing and chemical reaction. The relative importance of these processes is characterized by the Damköhler number, Da, which is the ratio of the rates of chemical reaction and fluid dynamic mixing. The extremes of the Damköhler number are designated as the "well-stirred" reactor (Da<<1) and the fast-chemistry (Da>>1) regimes, and at each extreme it is the slower process that limits or controls the behavior of the system. In the "well-stirred" reactor regime, the reactants and products rapidly mix, and the chemical reactions proceed over an extended region of the reactor on a time scale that is much longer than the mixing time. In contrast, the fast-chemistry regime is characterized by thin reaction zones, in which reactions proceed to completion as soon as the reactants come in contact, such that the rate of conversion of reactants to products is limited by the rate of mixing. The early theoretical work of Burke and Schumann modeled laminar nonpremixed flames as thin sheets using assumptions of an infinitely fast irreversible one-step reaction (Da=∞).6 The next improvement on this simplified model assumed infinitely fast reversible combustion reactions with the species and temperature at each location in the flame determined by local thermochemical equilibrium conditions. Turbulent non-premixed flames, however, exhibit significant non-equilibrium behavior and involve a wide range of Damköhler numbers. The turbulent flow field produces temporal and spatial fluctuations in the mixing rates, which induce local fluctuations in the chemical reaction rates. Further advances in modeling have sought to account for non-equilibrium and finite-rate chemistry effects that occur when the relevant Damköhler number is near unity. 1-4,7

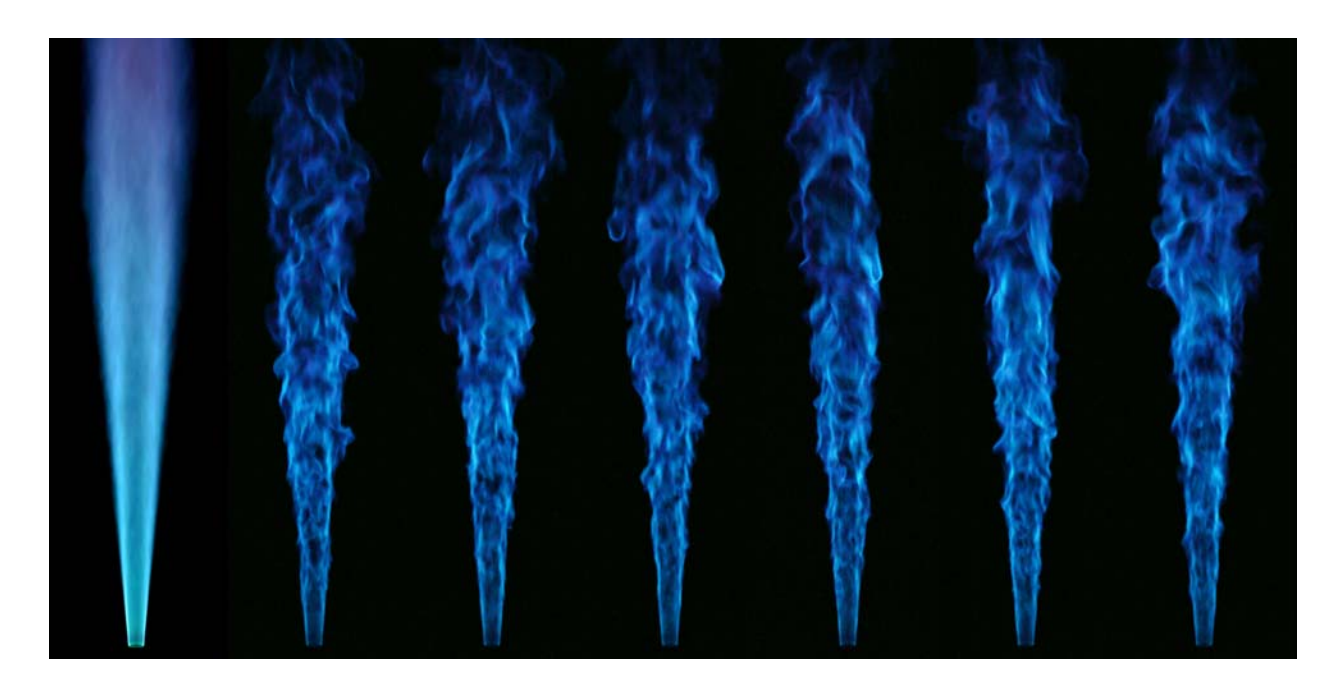


Figure 1. Chemiluminescence images of a turbulent  $CH_4/H_2/N_2$  jet flame ( $Re_d = 15,200$ ) measured with two different exposure times. The long exposure image (far left) indicates the mean flame structure, and the six shorter exposures to the right illustrate the instantaneous turbulent structure.

Jet flames provide a simple canonical geometry for illustrating essential features of turbulent non-premixed flames. In Fig. 1, chemiluminescence images, using different camera exposure times, show the mean and fluctuating structure of a turbulent non-premixed jet flame. The fuel is a  $N_2$ -diluted mixture of  $CH_4$  and  $H_2$  that issues from the jet at an exit Reynolds number of  $Re_d = Ud/v = 15,200$ , where U is the bulk exit velocity, d = 7.2 mm is the nozzle diameter, and v is the kinematic viscosity. This particular flame has been the object of many experimental studies over the past 10 years, beginning with work by Bergmann et al.<sup>8</sup>, and using a variety of measurement techniques in several laboratories around the world.<sup>9</sup> The long-exposure image on the left of the figure shows the mean envelope of the reaction zone, which is distributed across the mixing layer of the jet and the coflow. The six short-exposure images illustrate the complex instantaneous structure of turbulent flames. The turbulent flow distorts the

shape of the flame and produces a convoluted reaction zone with a wide range of length scales. These perturbations to the flame can result in significant variations in the local reaction rates. The reaction rates are highly non-linear functions of the temperature, so measurements of the mean thermochemical properties of the flame are not adequate for predicting the production rates of intermediate species and pollutants.

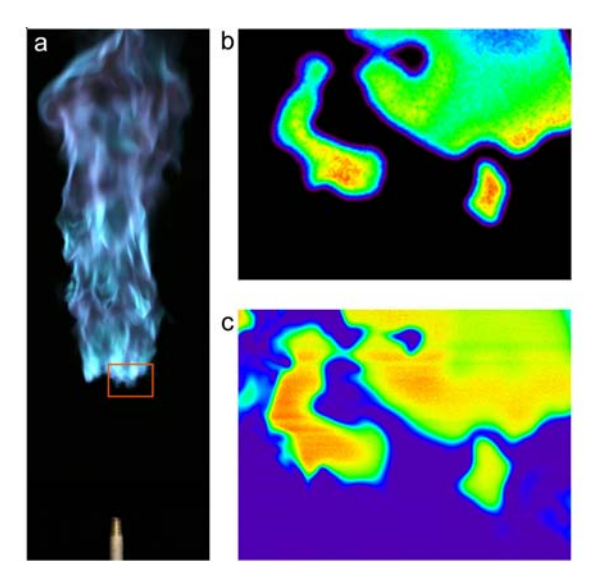


Figure 2. a) Chemiluminescence image of a turbulent lifted  $CH_4/H_2/N_2$  jet flame stabilized above the burner nozzle. The orange rectangle approximates the imaged area for b) OH-LIF measurements, and c) temperature measurements by Rayleigh scattering.

As the jet exit velocity is increased, the flame becomes increasingly turbulent but remains anchored to the rim of the burner nozzle. For sufficiently large jet velocities, however, the flame lifts off and stabilizes downstream of the nozzle, as is illustrated in Fig. 2a. The distance between the flame stabilization location and the nozzle exit is referred to as the lift-off height. Partial premixing of the fuel and oxidizer occurs in the region upstream of the flame stabilization location, such that the stabilization region consists of a turbulent edge flame that propagates against the flow of a nonuniform mixture of fuel and air. An example of this complex flame

structure is shown by the simultaneous OH-LIF and temperature measurements in Fig. 2. This stabilization region has some characteristics of both non-premixed and premixed flames, and this presents a challenge for combustion models. The lift-off height fluctuates as the local flow conditions vary in the turbulent jet. Detailed discussions of the stabilization mechanism of lifted flames are available elsewhere.<sup>2,10-12</sup>

If the jet velocity is increased further, after establishing a lifted flame, the flow reaches a condition for which a flame cannot be stabilized, and global extinction ensues. The velocity at which the flame extinguishes depends on the fuel composition and the degree of partial premixing. Global flame extinction is to be avoided in both fundamental research and practical applications, and many approaches have been developed to stabilize flames. For the flames in Figs. 1 and 2, the use of H<sub>2</sub> in the fuel mixture significantly increases the blow-off velocity relative to a CH<sub>4</sub>/N<sub>2</sub> fuel mixture. Alternative approaches to increasing the robustness of methane jet flames include partial premixing with an oxidizer and the use of pilot flames to help anchor the jet flame to the nozzle. Figure 3 shows an example of a partially premixed CH<sub>4</sub>/air (1/3 by vol.) jet flame anchored by an annular pilot of lean premixed flames. At these flow conditions, the fuel-rich premixed chemistry is too slow to significantly affect the flame structure, and the flame behaves as a non-premixed flame, with a single reaction zone. Such flames may be operated at higher exit velocities and higher Reynolds numbers than corresponding simple jet flames, and they have been used extensively for investigations of finiterate chemistry effects and the development of models that account for these effects.<sup>4,9</sup>



Figure 3. Chemiluminescence images of a turbulent partially-premixed CH<sub>4</sub>/air jet flame stabilized by premixed pilot flames.

# Mixture Fraction, Dissipation, and Finite-Rate Chemistry

The state of mixing between the fuel and oxidizer streams in non-premixed flames is quantified by the mixture fraction,  $\xi$ . Conceptually, the mixture fraction is the fraction of mass that originated in the fuel stream, with zero corresponding to the oxidizer stream and 1.0 corresponding to the pure fuel stream. The stoichiometric mixture fraction,  $\xi_{st}$ , indicates the condition for which the fuel and oxidizer are mixed in stoichiometric proportions. If a non-premixed flame is modeled as a two-stream mixing problem with assumptions of fast chemistry, equal diffusivities of all species, and unity Lewis number (the ratio of thermal diffusivity to mass diffusivity), the species mass fractions can be expressed solely as a function of the mixture fraction. The scalar dissipation rate, which is defined as  $\chi = 2D_{\xi}(\nabla \xi \cdot \nabla \xi)$ , where  $D_{\xi}$  is the corresponding diffusivity, quantifies the rate of molecular mixing and is prominent in the theory

and modeling of turbulent non-premixed combustion. The reaction rates are proportional to the scalar dissipation rate via the following relationship:  $w_i = -\rho \frac{\chi}{2} \frac{\partial^2 Y_i(\xi)}{\partial \xi^2}$ , where  $w_i$  is the chemical production rate of species i,  $\rho$  is the density, and  $Y_i(\xi)$  is the mass fraction of species i as a function of mixture fraction.<sup>13</sup>

The determination of mixture fraction in flames is challenging because it requires simultaneous measurements of all major species. Mixture fraction measurement techniques use combinations of Raman scattering, Rayleigh scattering, and laser-induced fluorescence (LIF). Multi-dimensional mixture fraction measurements are needed to determine the scalar dissipation. During the past two-and-a-half decades, the diagnostic capabilities for measuring mixture fraction in turbulent non-premixed flames have evolved significantly, as described by Frank et al. <sup>14</sup> and references therein. The application of these techniques to a range of burner geometries has provided important insights into turbulent non-premixed flames, and well-documented data sets are currently used for the development and validation of turbulent combustion models via the Turbulent Non-premixed Flame (TNF) Workshop. <sup>15</sup>

One of the most challenging aspects of modeling turbulent combustion is the accurate prediction of finite-rate chemistry effects. In highly turbulent flames, the local transport rates for removal of combustion radicals and heat can be comparable to or larger than the production rates of radicals and heat from combustion reactions. As a result, the chemistry cannot keep up with the transport, and the flame is quenched. To illustrate these finite-rate chemistry effects, we compare temperature measurements in two piloted, partially-premixed CH<sub>4</sub>/air (1/3 by vol.) jet flames with different turbulence levels. Figure 4 shows scatter plots of temperature as a function of mixture fraction for a fully burning flame (Flame C) and a flame with significant local

extinction (Flame F) at a downstream location of x/d=15.<sup>16</sup> These scatter plots provide a qualitative indication of the probability of local extinction, which is characterized by samples with strongly depressed temperatures. In Flame C, there is a very small probability of extinction, and the bulk of the data points are distributed along the curve that is obtained from a laminar flame calculation with a strain parameter of  $a = 100 \, \text{s}^{-1}$ . In contrast, Flame F has a high probability of localized extinction with a significant fraction of samples exhibiting reduced temperatures. Accurate modeling of localized extinction and reignition is important for the development of practical combustion devices with low pollutant emissions and stable operating conditions.

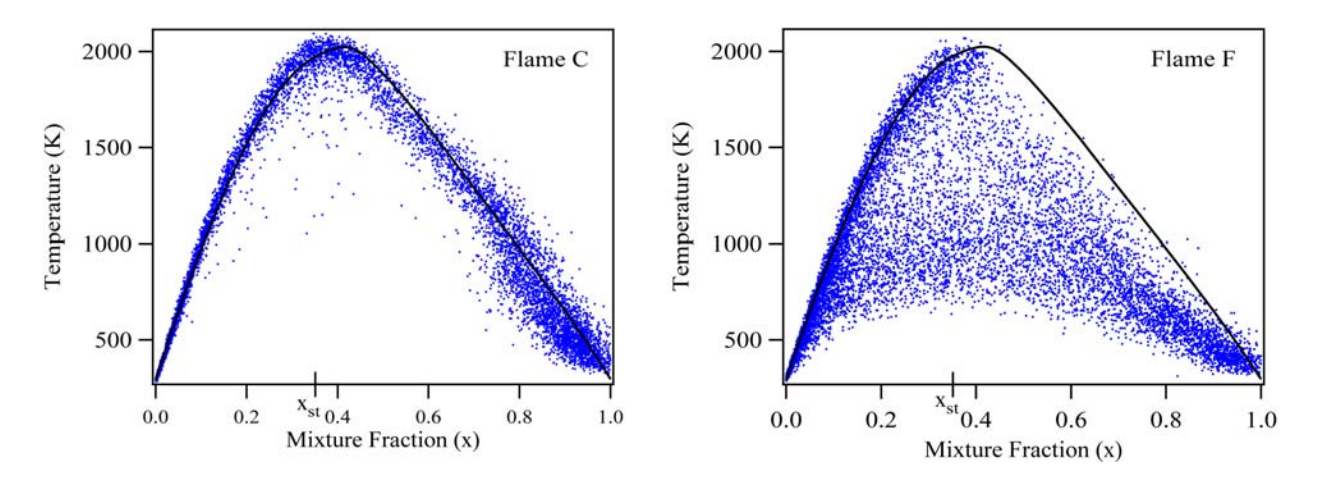


Figure 4. Scatter plots of temperature at x/d = 15 in turbulent CH<sub>4</sub>/air jet flames with Reynolds numbers of 13,400 (Flame C) and 44,800 (Flame F). The stoichiometric mixture fraction is  $\xi_{st} = 0.351$ . The line shows results of a laminar counterflow flame calculation with a strain parameter of  $a = 100 \text{ s}^{-1}$  and is included as a visual guide (From Barlow, R.S. and Frank, J.H. *Proc. Combust. Inst.*, 27, 1087, 1998. With permission).

Figure 5 provides a visualization of a localized extinction event in a turbulent jet flame using a temporal sequence of OH planar laser-induced fluorescence measurements. The OH-LIF measurements combined with particle image velocimetry (PIV) reveal that a distinct vortex

within the turbulent flow distorts and then breaks the OH front. These localized extinction events occur intermittently as the strength of the coupling between the turbulent flow and the flame chemistry fluctuates. As the frequency of these events increases, the characteristics of the turbulent flame can be significantly altered.

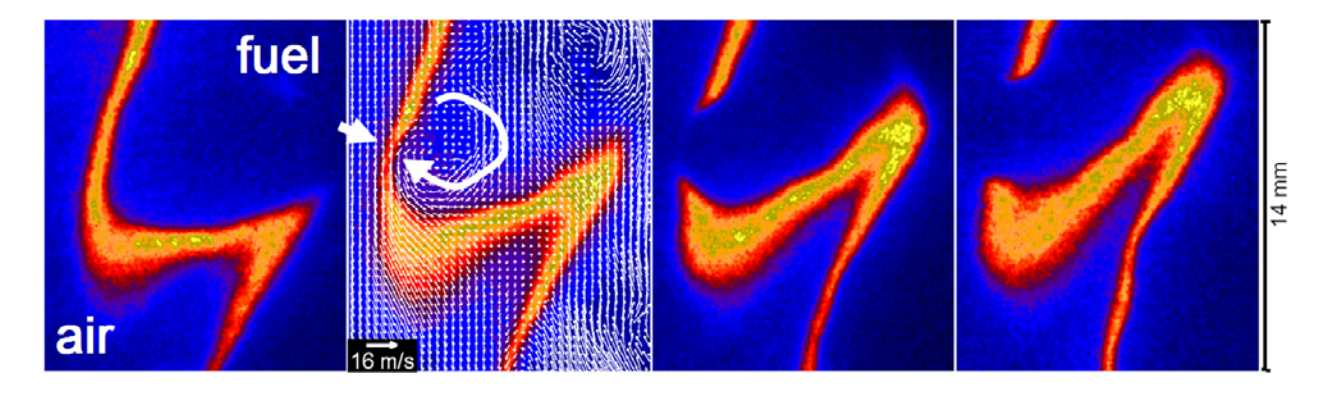


Figure 5. Temporal sequence of OH-LIF measurements captures a localized extinction event in a turbulent non-premixed  $CH_4/H_2/N_2$  jet flame (Re ~ 20,000) as a vortex perturbs the reaction zone. The time between frames is 125  $\mu$ s. The velocity field from PIV measurements is superimposed on the second frame and has the mean vertical velocity of 9 m/s subtracted (From Hult, J. et al., Paper No. 26-2, in 10th International Symposium on Applications of Laser Techniques to Fluid Mechanics, Lisbon, 2000. With permission.)

Experiments and large eddy simulations of turbulent jet flames have revealed thin sheet-like structures of high strain rate and high scalar dissipation rate that tend to be inclined to the flow, as shown in Fig. 6. Two-dimensional imaging measurements of scalar dissipation in a piloted jet flame, obtained using the methods described by Frank et al.<sup>14</sup>, are compared qualitatively with simulations of instantaneous scalar dissipation fields from two different LES models of a similar piloted jet flame, and the inclined structures of high scalar dissipation are evident in each frame. The importance of these structures to the overall combustion process is not fully understood and is the subject of ongoing research. However, there is evidence that local extinction may be caused by such structures and that a disproportionate amount of heat

release may occur in these structures, relative to the volume they occupy. Therefore, combustion models may have to account for the effects of these structures in order to accurately predict some combustion phenomena.

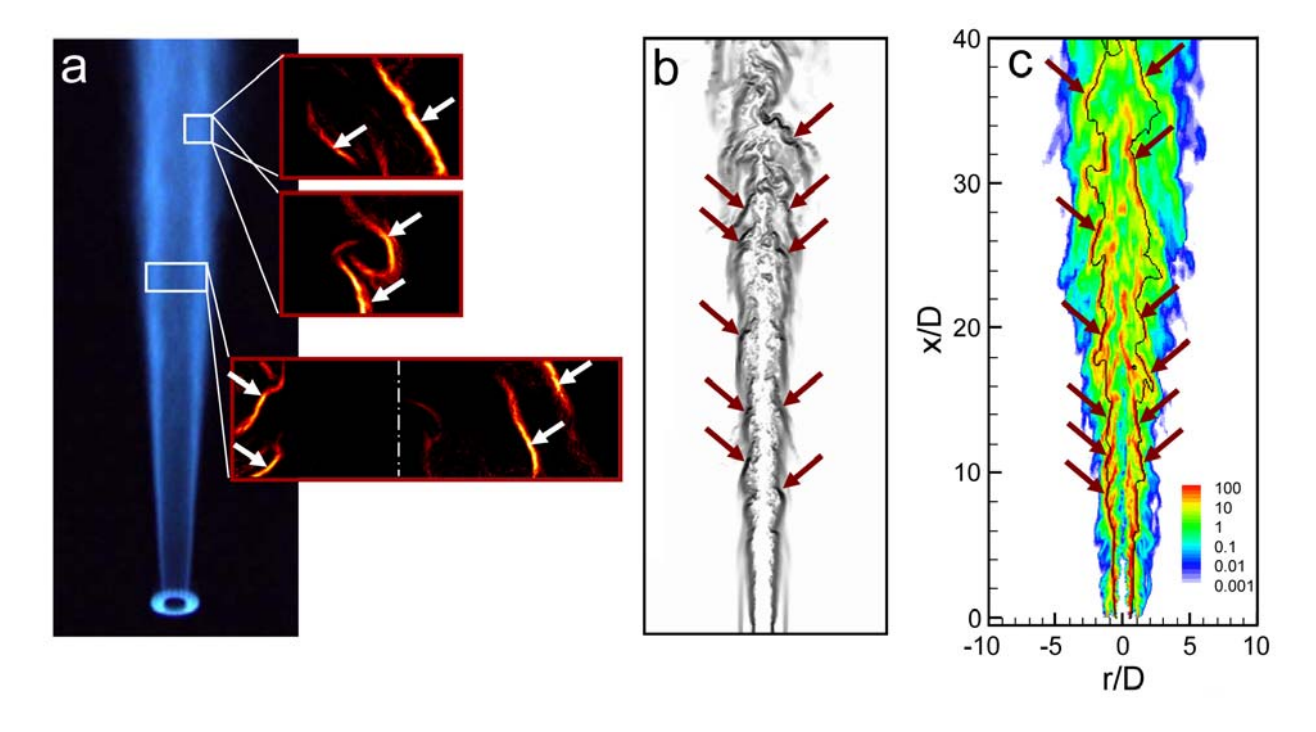


Figure 6 Qualitative comparison of the inclined structure of thin layers of high scalar dissipation in a piloted CH<sub>4</sub>/air jet flame as revealed by: a) mixture fraction imaging (Adapted from Frank et al., *Combust. Flame*, 143, 507-523, 2005. With permission.), b) LES with a steady flamelet library (Adapted from Kempf et al., *Proc. Combust. Inst.*, 30, 557-565, 2005. With permission.), and c) LES with unsteady flamelet modeling (Adapted from Pitsch, H. and Steiner, H., *Proc. Combust. Inst.*, 28, 41, 2000. With permission.)

### **Turbulence Structure and Length Scales**

Turbulent non-premixed flames contain a wide range of length scales. For a given flame geometry, the largest scales of turbulence are determined by the overall width of an unconfined jet flame or by dimensions of the hardware that contain the flow. Therefore, the largest scales of turbulent motion are typically independent of Reynolds number. As the Reynolds number increases, turbulent fluctuations in the velocity and mixture fraction cascade down to

progressively smaller eddies, increasing the dynamic range of the length scales. This extension to smaller scales is illustrated in Fig. 7 by OH-LIF measurements in turbulent H<sub>2</sub>/Ar jet flames with Reynolds numbers ranging from 30,000 to 150,000. The largest length scales of the OH regions are comparable across the three sets of images, but with increasing Reynolds number there is more fine-scale structure on the boundaries and within these large-scale structures.

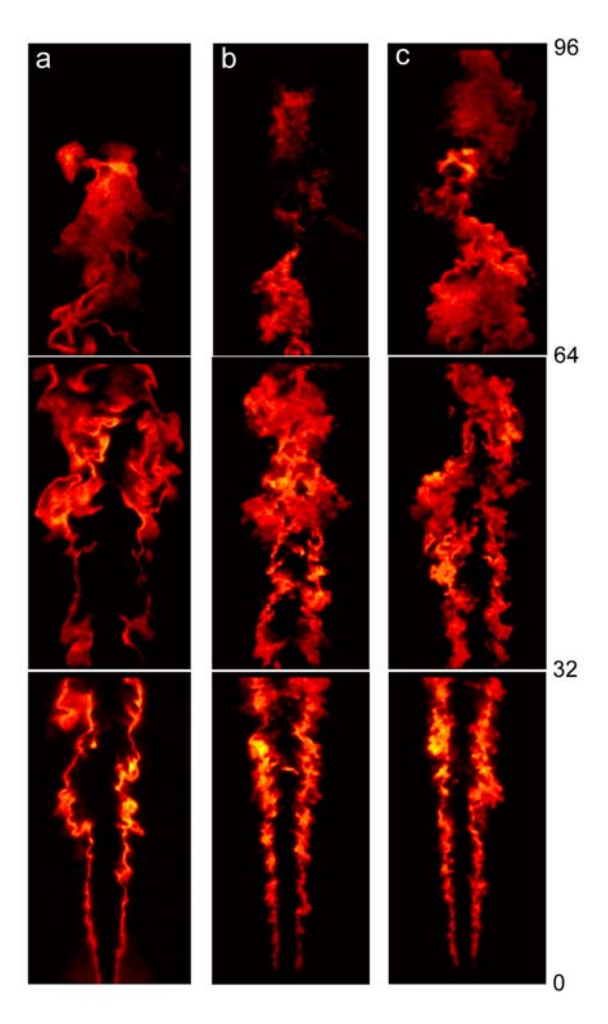


Figure 7. Composite OH laser-induced fluorescence images of turbulent non-premixed  $H_2/Ar$  jet flames with Reynolds numbers of (a)  $Re_d = 30,000$ , (b)  $Re_d = 75,000$ , and (c)  $Re_d = 150,000$ . Numbers on right indicate the streamwise distance in nozzle diameters (d = 5 mm). (Adapted from Clemens, N.T. et al., *Combust. Sci. Technol.*, 129, 165, 1997. With permission)

The chemical reactions that drive combustion can occur only after reactants have been mixed at the molecular level by diffusion. While turbulent transport, or "stirring", takes place

over a wide range of length scales, this final molecular mixing process is left to the smallest scales of turbulence, called the dissipation range. Based upon knowledge of non-reacting turbulent flows, we expect that experimental resolution must approach the smallest scales of turbulence for measurements of the mean scalar dissipation rate to be accurate. The relevant length scale for determining the local resolution requirement is the Batchelor scale,  $\lambda_B$ . This scale represents in an average sense the smallest length over which turbulent fluctuations in a scalar quantity, such as mixture fraction or temperature, can occur. Scalar fluctuations at length scales near the Batchelor scale are rapidly dissipated by diffusion and must be continually fed by "energy" from turbulent fluctuations at larger scales. (The corresponding scale for velocity fluctuations is the Kolmogorov scale,  $\eta$ .) Methods for estimating the Kolmogorov and Batchelor scales have been developed for non-reacting flows, but the applicability of such estimates to flames has been uncertain because relatively little is known about the structure of small-scale turbulence in reacting flows.

Recent research has significantly improved our quantitative understanding of the structure of non-premixed jet flames at the smallest scales of turbulence. Simultaneous line imaging of Raman scattering, Rayleigh scattering, and two-photon laser-induced fluorescence of CO has been used to investigate the energy and dissipation spectra of turbulent fluctuations in temperature and mixture fraction. When properly normalized, as in Fig. 8, the measured spectra for temperature fluctuations at various flame locations have the same shape in the dissipation range as the model spectrum of Pope 19 for turbulent kinetic energy dissipation in non-reacting flows. This similarity enables determination of a cutoff wavenumber,  $\kappa\lambda_B = \kappa_1^* = 1$ , in the 1-D dissipation spectrum. The local length scale inferred from this cutoff is analogous to the Batchelor scale in non-reacting flows. Furthermore, with Lewis number near

unity in these flames, the 1-D dissipation spectra for temperature and mixture fraction follow nearly the same roll off. These results represent a breakthrough in the development of quantitative diagnostics for scalar dissipation measurements in flames because they suggest that local resolution requirements may be determined for complex flames using the relatively simple technique of Rayleigh scattering.

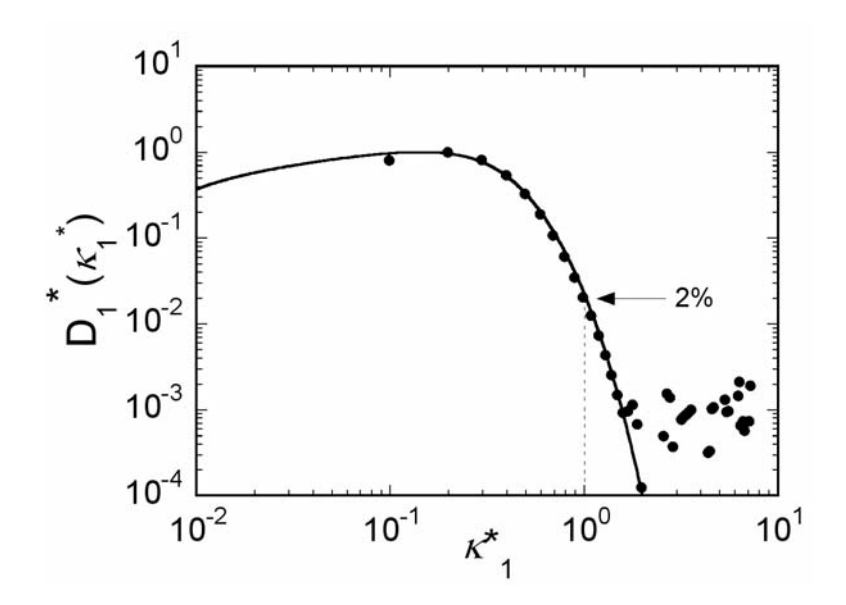


Figure. 8 Model 1-D dissipation spectrum from Pope<sup>19</sup> (line) and measured, noise-corrected spectrum of the radial gradient squared of fluctuating temperature in a  $CH_4/H_2/N_2$  jet flame ( $Re_d = 15,200$ ) (symbols). Each spectrum is normalized by its maximum value. The arrow indicates the 2 percent level, which corresponds to the normalized wavenumber  $\kappa_1^* = 1$  according to the model spectrum. (From Barlow, R.S., *Proc. Combust. Inst.*, 31, 49, 2007. With permission.)

High-resolution 2-D Rayleigh scattering imaging in turbulent jet flames has revealed intricate layered structures of high thermal dissipation and has provided measurements of dissipation spectra and length scales in both the radial and axial directions.<sup>20,21</sup> The spatial resolution that is required to resolve the thin layered structures is greater than the resolution that is needed to measure the mean dissipation, and these measurements give new insight into the detailed structures of the dissipation field. Figure 9 shows samples of single-shot temperature

and thermal dissipation measurements in the near field of a  $CH_4/H_2/N_2$  jet flame ( $Re_d = 15,200$ ). The variations in the thickness and spatial orientation of the dissipation structures reflect the interaction of the flame heat release and the turbulent jet flow. The low-temperature gases near the jet centerline at these upstream locations exhibit small turbulent structures with relatively isotropic orientations. In contrast, the high-temperature regions contain larger scale structures with a preferred orientation. Consequently, the contributions of axial and radial temperature gradients to the dissipation field are similar near the jet centerline but differ significantly in the high-temperature regions of the jet flame.

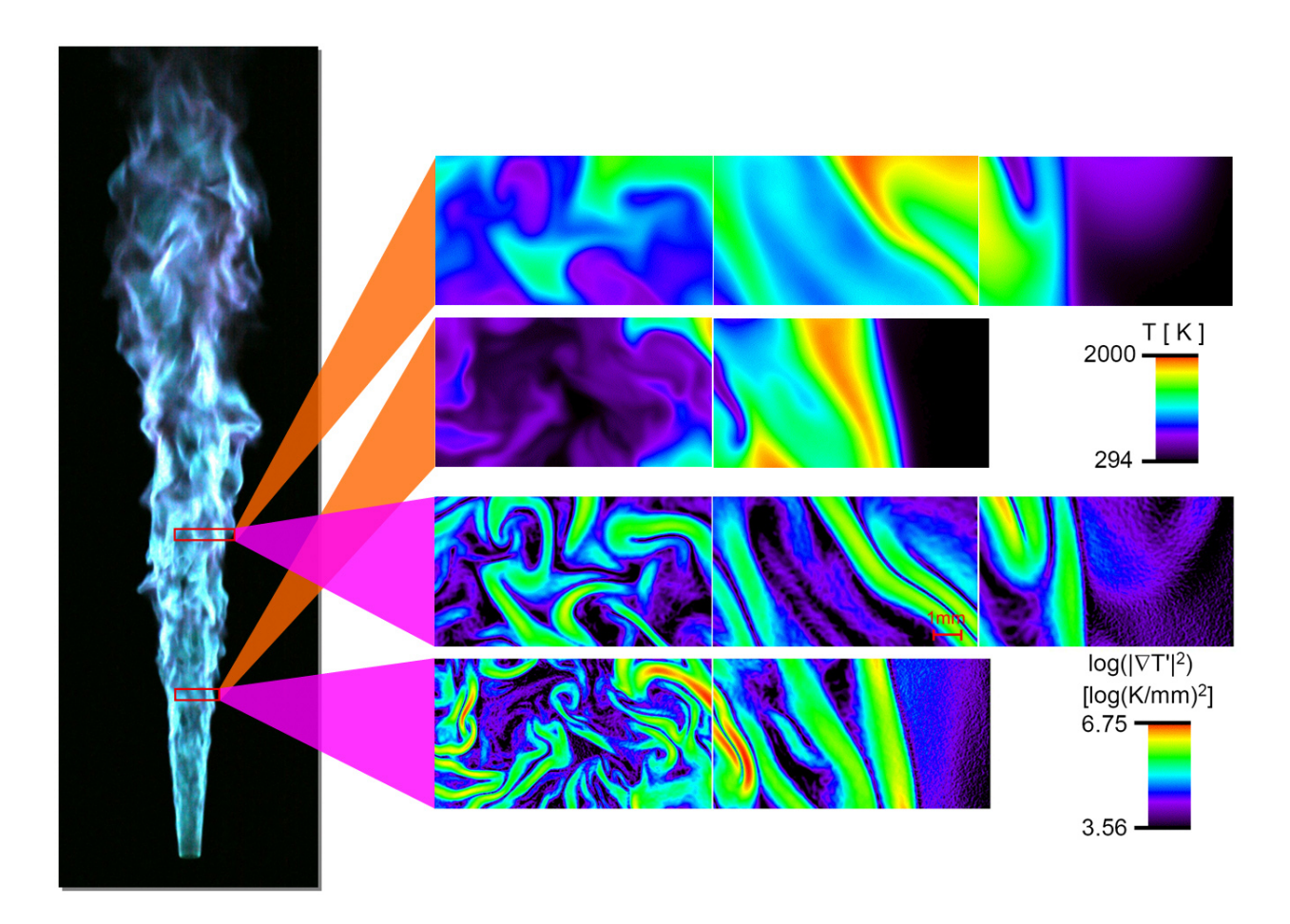


Figure 9. Instantaneous temperature and thermal dissipation measurements in a  $CH_4/H_2/N_2$  jet flame ( $Re_d = 15,200$ ) at x/d=10 and 20. The thermal dissipation is displayed on a log scale to show the wide dynamic range.

The ability to resolve the dissipation structures allows a more detailed understanding of the interactions between turbulent flows and flame chemistry. This information on spectra, length scales, and the structure of small-scale turbulence in flames is also relevant to computational combustion models. For example, information on the locally measured values of the Batchelor scale and the dissipation layer thickness may be used to design grids for large-eddy simulation (LES) or evaluate the relative resolution of LES results. There is also potential to use high-resolution dissipation measurements to evaluate subgrid scale models for LES.

### **Complex geometries**

Advancements in our fundamental understanding of turbulent non-premixed combustion through studies of simple canonical burner geometries are essential for developing and validating computational models that can predict the effects of interactions between turbulence and chemistry in flames. However, practical combustion devices often use complex burner geometries with swirling and recirculating flows that stabilize intense, highly turbulent flames with very high power densities. Consequently, the combustion research community has directed significant effort toward detailed studies of flames and burners that have recirculating flows, swirling flows, and stabilization of detached flames by mixing with combustion products at high temperatures. Two examples are described here, and some additional examples are outlined by Barlow.

One method of stabilizing a flame in a high velocity flow of air is to trap combustion products in the recirculation zone downstream of a bluff body. The extended residence time of the recirculating flow allows time for combustion reactions to proceed, and the high temperature

products then serve as a stable ignition source for the flame. Figure 10 shows a photograph of a bluff body flame of  $CH_4/H_2$  (equal parts by volume) and three computationally generated views of the structure of the recirculation zone. Fuel is injected through a 3.6-mm tube at the center of the bluff body, which is 50 mm in diameter and is surrounded by an air flow of up to 40 m/s.<sup>22</sup> The white rectangle in Fig. 10a indicates the region represented in Figs. 10b-d, which are obtained from LES.<sup>23</sup> The streamlines in Fig. 10b show the time averaged structure of the recirculation zone, which has two annular vortices. Figure 10c is generated by integrating an instantaneous line-of-sight view of the simulated OH radical concentration. , and in movie form they can yield useful insights on the dynamics of complex turbulent flames. Figure 10d shows a simulated instantaneous temperature field and provides an indication of the range of resolved length scales in this flame.

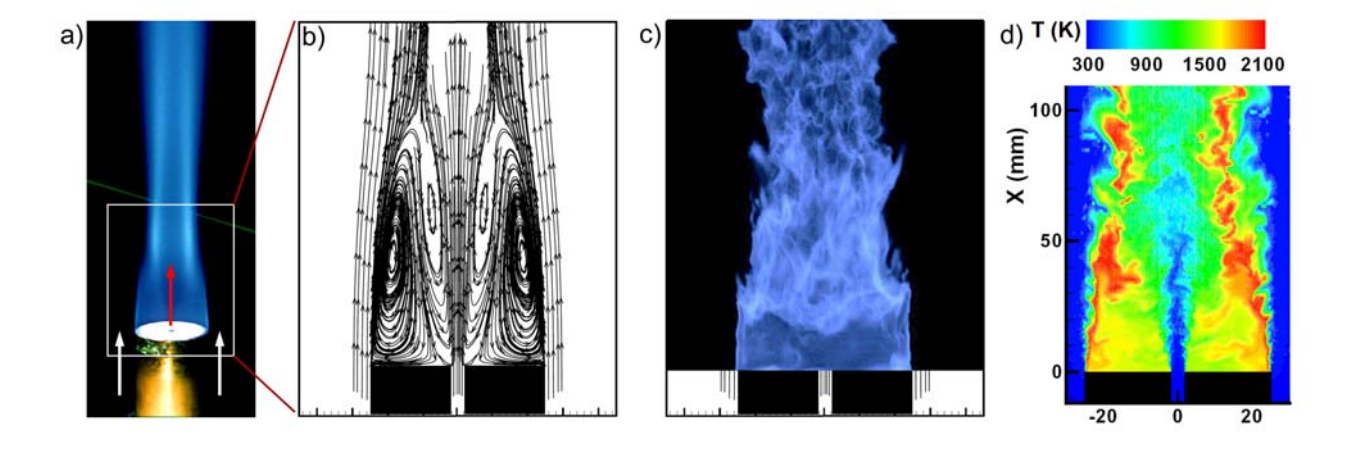


Figure 10. A bluff-body stabilized flame of CH<sub>4</sub>/H<sub>2</sub> in air (designated HM1 by Dally et al.<sup>22</sup>): a) time averaged photograph of flame luminosity, b) time average streamlines from LES, c) instantaneous visualization of OH "luminosity" from LES, and d) instantaneous temperature field from LES. (b and d are adapted from Raman, V., and Pitch, H., *Combust. Flame*, 142, 329, 2005. With permission.)

Bluff body flames can also exhibit local extinction, and the combination of recirculating

flow, large-scale dynamics, and local extinction is a contemporary challenge for advanced combustion models. However, these flames are still much simpler than those in a gas turbine combustor, for example. There is strong motivation to perform detailed experiments on non-premixed and partially premixed burners that include features of practical combustors. One such research target is the model gas turbine combustor shown in Fig. 11. This burner is designed to operate on gaseous fuels at atmospheric pressure. However, it is modeled after a liquid-fueled combustor used in small gas turbine engines. Two annular swirling flows of air surround a ring that injects fuel. The turbulent flame spreads out as a cone, and there are inner and outer recirculation zones. Detailed measurements of species and temperature have shown that the flame is detached from the injector and that a significant degree of mixing between fuel and air occurs before combustion.<sup>24</sup> Combustion products from the inner and outer recirculation zones are also entrained into this mixing region just above the fuel injector.

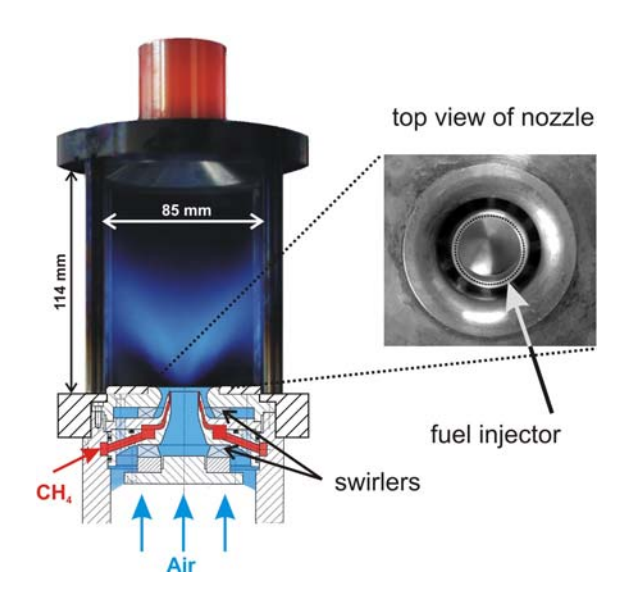


Figure 11. Diagram and photograph of a model gas turbine combustor operating on CH4 and air at atmospheric pressure. Fuel is injected from an annulus separating two swirling air streams. (From Wolfgang Meier. See supporting research in Meier, W. et al., *Combust. Flame*, 144, 225, 2006)

Figure 12 shows scatter plots of instantaneous measurements of temperature and CH<sub>4</sub> mole fraction obtained at a height of 5 mm and at several radial locations, which are color coded in the figure. The first things to notice are that there are no samples richer than 0.2 in mixture fraction (1.0 being pure fuel) and that many samples remain at room temperature even within the limits of flammability. Many samples also show an intermediate progress of reaction, with temperatures well below the calculated equilibrium (black) or strained laminar flame (orange) curves. These unreacted and partially reacted samples are from the highly strained mixing region above the injector jets. For measurement locations near the centerline (r = 0-2 mm) or outside the mixing layer (r = 16-30 mm) many samples are fully reacted and close to the equilibrium lines in the figures. These locations are in the inner and outer recirculation zones respectively, where mixing rates are slower compared to the chemical reaction rates.

In this burner configuration, fuel is injected directly into the combustion chamber, so one would initially categorize it as a non-premixed burner. However, the overall combustion process is quite complex and involves features of non-premixed, partially-premixed, and stratified combustion, as well as the possibility that auto-ignition of hot mixtures of fuel, air, and recirculated combustion products may play a roll in stabilizing the flame. Thus, while one may start from simple concepts of non-premixed turbulent flames, the inclusion of local extinction or flame liftoff quickly increases the physical and computational complexity of flames that begin with non-premixed streams of fuel and oxidizer.

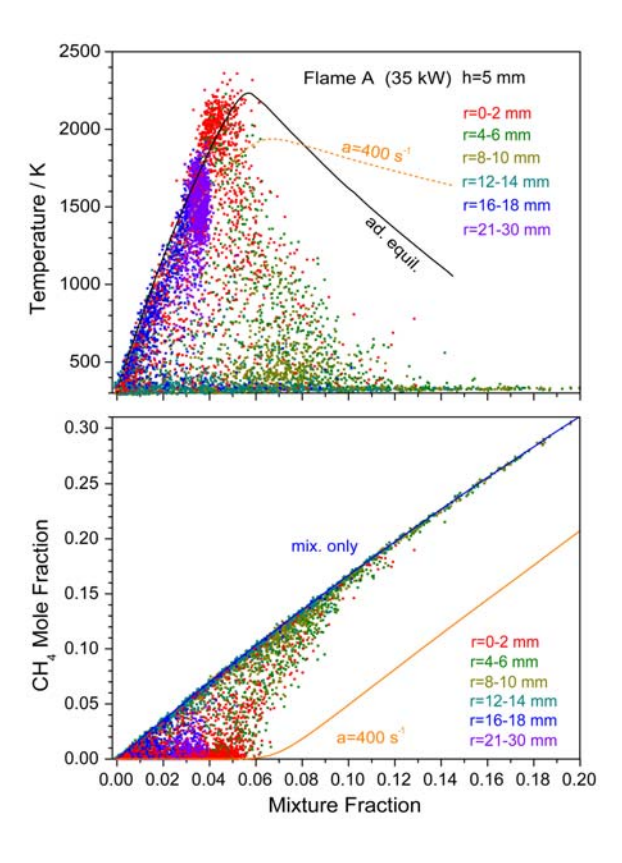


Figure 12. Scatter plots on temperature and CH<sub>4</sub> mole fraction vs. mixture fraction in a model gas turbine combustor. (From Meier, W. et al., *Combust. Flame*, 144, 225, 2006. With permission.)

## **Summary**

Here we have described some of the basic characteristics of non-premixed flames and provided a few examples of both simple and moderately complex flames and burner geometries for turbulent non-premixed combustion. The central theme in non-premixed combustion is that the structure and stability of a given flame depend on the coupling between turbulent mixing and chemical reactions. Mixture fraction (the state of mixing between fuel and oxidizer) and scalar dissipation (the rate of mixing at the molecular level) were identified as central concepts and quantities. Local extinction, flame liftoff and stabilization, length scales of turbulent flames, and the structure of thin dissipation layers were discussed as examples of important interactions of fluid dynamics and chemistry. Piloted flames, bluff body flames, and swirling flames were used

to illustrate a range of methods for stabilized flames in which the turbulent mixing rates are competitive with the critical rates of combustion reactions. These examples point toward the very complex nature of combustion in practical systems.

Non-premixed combustion will continue to be important for many applications in power generation, transportation, and industrial processing. The need to develop advanced combustion systems with high efficiency and very low pollutant emissions places increasing demands on computational design tools. Models for turbulent combustion systems will be predictive only if their underlying assumptions are soundly based in science and they have been validated against well-documented test cases. Much of what is currently known about turbulent non-premixed flames is based upon experiments using non-intrusive laser diagnostic techniques. However, due to rapid advancements in computational hardware and methods for detailed simulation of flames, direct numerical simulation (DNS) and highly resolved large eddy simulation (LES) are playing ever greater roles in fundamental research (Westbrook et al.<sup>25</sup>, Oefelein et al.<sup>26</sup>). The combination of closely coupled experiments and simulations is expected to significantly accelerate the development of predictive models for complex combustion systems over the next several years.

#### References

- <sup>1</sup> Bray, K. N. C., The Challenge of Turbulent Combustion, *Proc. Combust. Inst.*, 26, 1, 1996.
- <sup>2</sup> Peters, N., *Turbulent Combustion* Cambridge University Press, Cambridge, UK, 2000.
- <sup>3</sup> Vervisch, L., Using numerics to help the understanding of non-premixed turbulent flames, *Proc. Combust. Inst.*, 28, 11, 2000.
- <sup>4.</sup> Bilger, R. W., Pope, S. B., Bray, K. N. C., and Driscoll, J. F., Paradigms in turbulent combustion research, *Proc. Combust. Inst.*, 30, 21, 2005.
- <sup>5</sup> Poinsot, T. and Veynante, D., *Theoretical and Numerical Combustion*, 2nd ed. Edwards, Philadelphia, 2005.
- <sup>6</sup> Burke, S. P. and Schumann, T. E. W., Diffusion Flames, *Proc. Combust. Inst.*, 1, 2, 1928.
- <sup>7.</sup> Pope, S. B., Computations of turbulent combustion: progress and challenges, *Proc. Combust. Inst.*, 23, 591, 1990.
- <sup>8</sup> Bergmann, V., Meier, W., Wolff, D., and Stricker, W., Application of spontaneous Raman and Rayleigh scattering and 2D LIF for the characterization of a turbulent CH4/H2/N2 jet diffusion flame, *Appl. Phys. B*, 66, 489, 1998.
- <sup>9</sup> Barlow, R. S., Laser diagnostics and their interplay with computations to understand turbulent combustion, *Proc. Combust. Inst.*, 31, 49, 2007.
- <sup>10.</sup> Su, L. K., Sun, O. S., and Mungal, M. G., Experimental investigation of stabilization mechanisms in turbulent, lifted jet diffusion flames, *Combust. Flame*, 144, 494, 2006.
- <sup>11.</sup> Muniz, L. and Mungal, M. G., Instantaneous flame-stabilization velocities in lifted-jet diffusion flames, *Combust. Flame*, 111, 16, 1997.
- <sup>12.</sup> Pitts, W. M., Assessment of theories for the behavior and blowout of lifted turbulent jet diffusion flames, *Proc. Combust. Inst.*, 22, 809, 1988.
- <sup>13</sup> Bilger, R. W., The Structure of Diffusion Flames, *Combust. Sci. Technol.*, 13, 155, 1976.
- <sup>14.</sup> Frank, J. H., Kaiser, S. A., and Long, M. B., Multiscalar imaging in partially premixed jet flames with argon dilution, *Combust. Flame*, 143, 507, 2005.
- <sup>15</sup> Barlow, R. S., Editor: International workshop on measurement and computation of turbulent nonpremixed flames in <a href="http://www.ca.sandia.gov/TNF2007">http://www.ca.sandia.gov/TNF2007</a>.
- <sup>16.</sup> Barlow, R. S. and Frank, J. H., Effects of Turbulence on Species Mass Fractions in Methane/Air Jet Flames, *Proc. Combust. Inst.*, 27, 1087, 1998.
- <sup>17</sup> Wang, G. H., Barlow, R. S., and Clemens, N. T., Quantification of resolution and noise effects on thermal dissipation measurements in turbulent non-premixed jet flames, *Proc. Combust. Inst.*, 31, 1525, 2007.
- <sup>18.</sup> Wang, G. H., Karpetis, A. N., and Barlow, R. S., Dissipation length scales in turbulent nonpremixed jet flames, *Combust. Flame*, 148, 62, 2007.
- <sup>19</sup> Pope, S. B., *Turbulent Flows* Cambridge University Press, New York, 2000.
- <sup>20.</sup> Frank, J. H. and Kaiser, S. A., High-resolution Rayleigh imaging of dissipative structures, *Exp. Fluids*, In press, 2007.

  <sup>21.</sup> Kaiser, S. A. and Frank, J. H., Imaging of dissipative structures in the near field of a turbulent
- <sup>21</sup> Kaiser, S. A. and Frank, J. H., Imaging of dissipative structures in the near field of a turbulent non-premixed jet flame, *Proc. Combust. Inst.*, 31, 1515, 2007.
- <sup>22.</sup> Dally, B. B., Masri, A. R., Barlow, R. S., and Fiechtner, G. J., Instantaneous and mean compositional structure of bluff-body stabilized nonpremixed flames, *Combust. Flame*, 114, 119, 1998.
- <sup>23.</sup> Raman, V. and Pitsch, H., Large-eddy simulation of a bluff-body-stabilized non-premixed

flame using a recursive filter-refinement procedure, *Combust. Flame*, 142, 329, 2005. <sup>24.</sup> Meier, W., Duan, X. R., and Weigand, P., Investigations of swirl flames in a gas turbine model combustor - II. Turbulence-chemistry interactions, Combust. Flame, 144, 225, 2006.

<sup>25</sup> Kempf, A., Flemming, F., and Janicka, J., Investigation of lengthscales, scalar dissipation, and flame orientation in a piloted diffusion flame by LES, Proc. Combust. Inst., 30, 2005.

<sup>26</sup> Oefelein, J. C., Schefer, R. W., and Barlow, R. S., Toward validation of large eddy simulation for turbulent combustion, AIAA Journal, 44, 418, 2006.